

## The crystal structure of parisite-(Ce), $\text{Ce}_2\text{CaF}_2(\text{CO}_3)_3$

YUNXIANG NI,<sup>1</sup> JEFFREY E. POST,<sup>1</sup> AND JOHN M. HUGHES<sup>2,\*</sup>

<sup>1</sup>Department of Mineral Sciences, NHB-119, Smithsonian Institution, Washington, D.C. 20560, U.S.A.

<sup>2</sup>Department of Geology, Miami University, Oxford, Ohio 45056, U.S.A.

### ABSTRACT

The crystal structure of parisite-(Ce) was solved and refined to  $R = 0.044$ ,  $R_w = 0.037$  using three-dimensional X-ray diffraction data (XRD). In contrast to the putative hexagonal cell, weak XRD maxima on precession films demonstrate that the parisite-(Ce) is monoclinic with a space group  $C2/c$  or  $Cc$ .

The unit cell was refined as  $a = 12.305(2)$ ,  $b = 7.1053(5)$ ,  $c = 28.250(5)$  Å, and  $\beta = 98.257(14)^\circ$ . The structure refinement confirmed the space group  $Cc$ . Like bastnäsite and synchysite, parisite possesses a (001) layer structure, with layers of (Ca) and (CeF) separated by layers of carbonate groups. The [001] layer stacking sequence is ... (Ca),  $(\text{CO}_3)$ , (CeF),  $(\text{CO}_3)$ , (CeF),  $(\text{CO}_3)$ , (Ca),  $(\text{CO}_3)$ , (CeF),  $(\text{CO}_3)$ , (CeF),  $(\text{CO}_3)$ , ...

The parisite-(Ce) structure can be considered as two portions of the bastnäsite structure connected by a (Ca) layer. The insertion of a (Ca) layer would create long [001]\* structure voids in the F columns if the bastnäsite portions stacked hexagonally; therefore, the two bastnäsite portions are offset along  $[\bar{1}10]$  by  $a/6(\sin 60^\circ)$  (or  $[1\bar{0}0]$  in hexagonal cells, by  $a/3$ ) such that the oxygen atoms of the vertical edges of the carbonate groups occupy the voids. Polytypism results because a bastnäsite portion can shift equally in two possible directions,  $\pm 120^\circ$  from the previous offset vector. The parisite-(Ce) structure elucidated herein is the simplest and most common polytype possible, 2M. The polytype 6R, which was previously believed to be the most common, has not been found during our extensive study.

### INTRODUCTION

Parisite-(Ce),  $\text{Ce}_2\text{CaF}_2(\text{CO}_3)_3$ , is a calcium rare earth (RE) fluorocarbonate mineral, along with bastnäsite, synchysite, and röntgenite. The RE fluorocarbonates have generated considerable interest because of the pervasive syntactic intergrowths among the phases and their economic importance as the principal ores of RE metals. Understanding the detailed crystal chemistry of the RE fluorocarbonate minerals will provide insight into the formation of RE mineral deposits that are the primary source of rare earth elements for industrial use.

The crystal structures of RE fluorocarbonate phases were first studied in detail by Oftdel (1931a, 1931b). Donnay and Donnay (1953) offered a crystal-chemical summary of the mineral series and, on the basis of X-ray precession photographs, elucidated three hexagonal subcells and a real hexagonal cell with  $c = 84.1$  Å for parisite. They predicted the positions of the heavy atoms and some atoms of the carbonate groups for parisite-(Ce), by analogy with other RE fluorocarbonate phases.

The parisite crystal structure, along with those of other Ca fluorocarbonate phases, resisted solution because of the “universal” (Donnay and Donnay 1953) syntactic intergrowths among the phases. Van Landuyt and Amelinckx (1975) concluded that it

was not possible to determine the details of the crystal structures of these minerals by XRD techniques because of the impossibility of obtaining a crystal free from intergrowths. Transmission electron microscopy (TEM) studies have revealed a variety of syntactic intergrowths that can be described as mixtures,  $B_m S_n$ , of bastnäsite [B;  $\text{Ce}(\text{CO}_3)\text{F}$ ] and synchysite [S;  $\text{CeCaF}(\text{CO}_3)_2$ ] (van Landuyt and Amelinckx 1975; Wu et al. 1998; Yang et al. 1994), which can well explain their chemical composition. In addition to the four most common mineral species of the series mentioned above, numerous other intergrowth domains have been reported on the basis of TEM studies (Yang et al. 1994; Wu et al. 1998). No domain has been found, however, with a greater Ca component than in synchysite. In addition, although TEM images reveal the stacking sequence of mixed layer domains,  $B_m S_n$ , the details of their atomic arrangements remain unclear; for example, the orientation and stacking sequences of the carbonate groups cannot be determined from the TEM images. The recent successful structure determinations of bastnäsite (Ni et al. 1993) and synchysite (Wang et al. 1994) have provided the first detailed structure information about the mineral group. In the present study we are able to continue that effort by reporting the crystal structure of an exceptional parisite-(Ce) crystal.

The solutions of the structures of bastnäsite-(Ce) and synchysite-(Ce) have revealed the features of the (001) layer structure and elucidated the geometry of each structural layer: the (CeF) layer, the (Ca) layer, and the  $(\text{CO}_3)$  layers. These layers each have hexagonal symmetry. Although bastnäsite is hexagonal,

\*E-mail: hughes@miaavx1.muohio.edu

synchysite is actually monoclinic with a pronounced pseudohexagonal cell; the symmetry breaking results from the (Ca) layers in synchysite. The insertion of those layers results in the shift of portions of the structure from hexagonal stacking to eliminate the voids created by the addition of the (Ca) layers (Wang et al. 1994). The solution of the synchysite atomic arrangement provides insight for unraveling the parisite atomic arrangement because parisite possesses similar (Ca) layers.

### EXPERIMENTAL METHODS

The crystal used in this study appeared to be a secondary growth within a small void in a 5 mm diameter, 10 mm high hexagonal-prismatic crystal of parisite-(Ce) from Muso mine, Colombia (NMNH no. 122145). Long-exposure precession photographs revealed sharp diffractions, even for weak spots, and no evidence of syntactic intergrowths. Detailed examination of a complete suite of precession photographs indicated that the true symmetry of this parisite-(Ce) is monoclinic, despite the pronounced hexagonal pseudosymmetry that earlier studies emphasized. The true monoclinic cell is related to the hexagonal pseudo-cell  $c'$  of Donnay and Donnay (1953) ( $a = 7.105$ ,  $c' = 28.25$  Å) by the matrix  $2,1,0/0,1,0/-0.667, -0.333, 1$ . Examination of the photographs taken about the  $\mathbf{a}_1$ ,  $\mathbf{a}_2$ , and  $\mathbf{a}_3$  "hexagonal" axes showed weak reflections in reciprocal lattice planes (100)\* that

are not equivalent among the axes, and revealed the monoclinic symmetry. Systematic absences indicated a  $C$ -centered cell and the presence of a  $c$ -glide plane, consistent with space groups  $C2/c$  or  $Cc$ . The crystal structure has been successfully refined in the accentric space group  $Cc$ , the space group in which synchysite crystallizes (Wang et al. 1994).

Analyses were performed on an ARL nine-spectrometer microprobe at the Smithsonian Institution, using fluorite (Ca, F) and synthetic monazite phases from the Oak Ridge Laboratories (REEs) as standards. Electron microprobe analyses were performed on four fragments of the same crystal as used for collection of the XRD data, and each grain was analyzed in at least four places. The results are listed in Table 1. The chemical formula shown in Table 2 was calculated from the average result. The sums of the analyses are all less than 100%, which could be attributed to many factors, such as undetected heavy REs. The microprobe analyses, however, confirm the homogeneity of the sample.

X-ray intensity data for parisite-(Ce) were collected on an Enraf-Nonius CAD4 diffractometer utilizing graphite-monochromated  $\text{MoK}\alpha$  radiation. Unit-cell parameters were refined (no symmetry constraints) using diffraction angles from 25 centered reflections (centering 4 positions for each reflection:  $\pm\theta$ ,  $\theta$ ,  $-\theta$ ,  $-\theta$ ).

**TABLE 1.** The results of electron microprobe analyses of parisite-(Ce) from Muso, Columbia

wt%	Grain no. 1	Grain no. 2	Grain no. 3	Grain no. 4	Average	Ideal
CaO	10.79(7)	10.64(8)	10.67(22)	10.71(16)	10.70	10.44
La <sub>2</sub> O <sub>3</sub>	14.94(9)	15.38(23)	14.89(27)	15.17(43)	15.10	
Ce <sub>2</sub> O <sub>3</sub>	28.89(28)	28.90(16)	28.83(15)	28.85(37)	28.87	60.89
Pr <sub>2</sub> O <sub>3</sub>	3.09(3)	2.96(20)	2.92(8)	3.02(4)	3.00	
Nd <sub>2</sub> O <sub>3</sub>	11.86(34)	11.79(16)	11.53(8)	11.43(26)	11.65	
Sm <sub>2</sub> O <sub>3</sub>	1.47(3)	1.49(11)	1.49(9)	1.40(7)	1.46	
Eu <sub>2</sub> O <sub>3</sub>	0.16(6)	0.17(4)	0.21(9)	0.25(6)	0.20	
F	5.10(36)	5.60(26)	5.67(13)	4.97(37)	5.34	7.07
CO <sub>2</sub> *	24.58	24.58	24.58	24.58	24.58	24.58
-F=O	2.14	2.35	2.38	2.08	2.24	2.98
Sum	98.74	99.16	98.41	98.30	98.65	100.00

\* CO<sub>2</sub> calculated assuming ideal stoichiometry.

**TABLE 2.** Crystal data and results of structure refinements for parisite-(Ce)

Occurrence	Muso Mine, Colombia (NMNH no. 122145)		
Dimension	0.12 × 0.12 × 0.10 mm		
Unit cell			
Least squares			
a (Å)	12.305(2)	a(°)	90.005(9)
b	7.1053(5)	β	98.257(14)
c	28.250(5)	γ	89.986(9)
Constrained (space group: Cc)			
a (Å)	12.3049	c	28.2478
b	7.1056	β(°)	98.2416
Composition	(Ce <sub>0.94</sub> La <sub>0.50</sub> Nd <sub>0.37</sub> Pr <sub>0.10</sub> Sm <sub>0.05</sub> ) <sub>1.96</sub> Ca <sub>1.02</sub> F <sub>1.51</sub> C <sub>3</sub> O <sub>9.21</sub>		
Z	12		
θ limit	0.4–31.0°		
Standards			
Intensity	3 per 9 h	Scan type	ω/2θ
Orientation	3 per 300 reflections	Scan time(s)	≤120 s
Data collected	7772	R <sub>merge</sub>	0.023
Unique data	3890	R	0.044
Data > 3σ <sub>i</sub>	2567	R <sub>w</sub>	0.037
Largest peaks on difference map (e/Å <sup>3</sup> )			
(+)	1.82	Variables	203
(−)	0.52		

Notes: Numbers in parentheses denote one ESD of least units cited.

Chemical formula is from average of analyses of four fragments of the crystal used for structure analysis.

±chi). The unit cell and crystal data are given in Table 2, with details of data collection and structure refinement.

The crystallographic package MolEN (Fair 1990) was used throughout the solution and refinement. Intensity data were reduced to structure factors and corrected for Lorentz and polarization effects. Absorption was corrected using 360°  $\psi$ -scan data for 11 reflections. Because of the high linear absorption coefficient of the phase, after solution we employed the absorption surface method as implemented in program DIFABS (Walker and Stuart 1983). Symmetry-equivalent reflections were averaged; unit weights,  $I > 3\sigma_I$  data, and neutral-atoms scattering factors with terms for anomalous dispersion were used throughout structure calculations. The phase problem for the heavy atoms was solved by using the prediction of Donnay and Donnay (1953) and by direct methods (MULTAN-80; Main et al. 1980). The difference Fourier maps revealed all remaining light atoms.

During early stages of the structure refinement, the thermal parameters of the Ca atoms were refined to relatively low values, suggesting that the electron occupancy described by the Ca scattering factors was not sufficient to describe the scattering contributed by the Ca sites. Ce was added to the Ca sites and the occupancies were refined to  $Ca_{0.97}Ce_{0.03}$  at Ca1,  $Ca_{0.98}Ce_{0.02}$  at Ca2, and  $Ca_{0.98}Ce_{0.02}$  at Ca3. Attempts to refine anisotropic thermal parameters led to non-positive-definite thermal ellipsoids for about 1/3 of the atoms. Thus, only isotropic temperature factors were used for the final cycle of the refinement. An extinction factor was also refined, and no attempt was made to model twinning in the structure.

Table 3 lists refined positional parameters, isotropic thermal parameters, and bond-valence sums for all atoms, and Table 4 presents selected bond-lengths for atoms in parisite-(Ce); Table 5 contains observed and calculated structure factors for parisite-(Ce).<sup>1</sup> Bond-valence sums (Brown 1981) are in good agreement with the formal valence, except for the atoms of a few carbonate groups such as C1 and C4. Considering the distance sensitivity of the calculated contribution of the C-O bonds to the valence sum, the deviation is attributed to the inaccuracy of the refined C-O bond distances in the carbonate groups.

### DESCRIPTION OF THE STRUCTURE

The atomic arrangement of parisite has long resisted determination, in part because of the pronounced pseudohexagonal symmetry. Our attempts at refinement in hexagonal space groups invariably terminated with the successful location of the heavy atoms but inability to locate the complete carbonate groups.

The pronounced pseudohexagonal cell of parisite-(Ce) is consistent with its crystal form. Donnay and Donnay (1953) presented a putative hexagonal subcell of  $a = 7.12 \text{ \AA}$  and  $c' = 28.05 \text{ \AA}$  [Oftedal (1931b) determined  $a = 4.11 \text{ \AA}$ , which is only correct for the heavy atom arrangement]. On the basis of weak

**TABLE 3.** Atomic coordinates, isotropic B value, and bond valence sum (BVS, valence units) for atoms in parisite-(Ce)

Atom	x	y	z	B ( $\text{\AA}^2$ )	BVS
Ce1	0.473	0.2448(1)	0.163	0.40(1)	3.02
Ce2	0.80237(7)	0.2519(2)	0.16344(3)	0.62(1)	3.10
Ce3	0.14029(6)	0.2547(1)	0.16362(3)	0.26(1)	3.06
Ce4	0.52991(8)	0.2433(1)	0.33671(4)	0.44(1)	3.06
Ce5	0.19867(6)	0.2522(1)	0.33687(3)	0.24(1)	3.15
Ce6	0.85919(7)	0.2487(2)	0.33632(3)	0.68(1)	3.01
Ca1	0.0838(2)	0.2600(4)	-0.0001(1)	0.24(3)	2.00
Ca2	0.4130(3)	0.2543(5)	0.9996(1)	0.29(3)	1.90
Ca3	0.7471(3)	0.2434(5)	0.0008(1)	0.32(3)	1.88
F1	0.970(1)	0.083(1)	0.1633(5)	0.8(1)	1.10
F2	0.2981(8)	0.082(1)	0.1481(4)	0.6(1)	1.11
F3	0.645(1)	0.084(2)	0.1799(5)	1.5(2)	1.15
F4	0.028(1)	0.080(1)	0.3384(5)	0.9(1)	1.10
F5	0.6904(8)	0.080(1)	0.3213(4)	0.6(1)	1.18
F6	0.368(1)	0.086(2)	0.3535(5)	1.5(2)	1.11
O11	0.390(1)	0.317(2)	0.0803(6)	1.6(2)	1.83
O12	0.243(1)	0.427(2)	0.0378(6)	1.4(2)	2.50
O13	0.264(1)	0.447(2)	0.1147(6)	1.9(3)	2.28
O21	0.098(1)	0.134(2)	0.0801(6)	1.1(2)	1.94
O22	0.591(1)	0.382(2)	0.0343(6)	1.9(3)	2.21
O23	0.621(1)	0.347(2)	0.1116(6)	1.5(2)	1.96
O31	0.838(1)	0.298(2)	0.0793(5)	1.2(2)	2.15
O32	0.985(1)	0.445(2)	0.1129(5)	1.1(2)	2.04
O33	0.941(1)	0.431(2)	0.0328(6)	1.4(2)	1.84
O41	0.106(1)	0.295(2)	0.2510(5)	1.1(2)	1.74
O42	0.959(1)	0.435(2)	0.2114(6)	1.7(3)	1.94
O43	0.985(1)	0.436(2)	0.2884(6)	1.7(2)	2.61
O51	0.836(1)	0.132(2)	0.2508(7)	1.8(3)	2.05
O52	0.348(1)	0.379(2)	0.2916(5)	1.1(2)	2.07
O53	0.324(1)	0.364(2)	0.2118(5)	1.0(2)	2.06
O61	0.555(1)	0.319(2)	0.2505(5)	0.8(2)	1.94
O62	0.700(1)	0.447(2)	0.2906(5)	1.0(2)	1.95
O63	0.679(1)	0.453(2)	0.2113(5)	0.9(2)	2.18
O71	0.951(1)	0.292(2)	0.4205(6)	1.8(3)	2.05
O72	0.079(1)	0.443(2)	0.3857(5)	0.6(2)	1.95
O73	0.0836(9)	0.432(2)	0.4678(4)	0.3(2)	1.85
O81	0.505(1)	0.315(3)	0.4218(7)	2.4(3)	11.64
O82	0.346(1)	0.449(2)	0.3899(6)	1.3(2)	2.29
O83	0.3961(9)	0.425(2)	0.4695(4)	0.3(2)	2.11
O91	0.710(1)	0.347(2)	0.3877(6)	1.1(2)	2.16
O92	0.211(1)	0.134(2)	0.4219(5)	0.9(2)	1.76
O93	0.737(1)	0.393(2)	0.4687(5)	0.7(2)	1.87
C1	0.293(2)	0.403(3)	0.0768(9)	1.8(3)	4.62
C2	0.608(1)	0.453(2)	0.0744(7)	0.6(2)	4.21
C3	0.920(1)	0.395(2)	0.0763(6)	0.2(2)	4.11
C4	0.012(2)	0.389(3)	0.252(1)	1.7(3)	4.40
C5	0.341(2)	0.453(3)	0.2505(8)	0.9(2)	4.29
C6	0.646(1)	0.407(2)	0.2492(7)	0.5(2)	4.16
C7	0.038(1)	0.393(2)	0.4234(6)	0.1(2)	3.79
C8	0.406(2)	0.403(3)	0.4258(8)	1.3(3)	4.11
C9	0.723(2)	0.447(3)	0.4240(8)	1.2(3)	3.87

Note: Numbers in parentheses denote 1 esd of last unit cited.

superstructure reflections, Donnay and Donnay (1953) and later authors proposed  $c = 3c' = 84.15 \text{ \AA}$  for an hexagonal cell, assuming space group  $R3$ . As noted above, careful examination of weak reflections in the precession photographs taken in this study revealed monoclinic symmetry for parisite-(Ce). Our monoclinic cell indexes all the weak reflections that Donnay and Donnay (1953) noted for the  $c = 3c' = 84.15 \text{ \AA}$  hexagonal cell. The weak reflections result from the orientation and stacking of carbonate groups in a manner non-orthogonal to (001); because of their weak scattering power relative to the heavy atoms in parisite-(Ce), the X-ray evidence for monoclinic symmetry is subtle. If the weak reflections from carbonate groups are neglected, the diffraction pattern can be indexed on an hexagonal cell with  $c = 28.10 \text{ \AA}$ .

Donnay and Donnay (1953) suggested that the fluorcarbonate

<sup>1</sup>For a copy of Table 5, document item AM-99-034, contact the Business Office of the Mineralogical Society of America (see inside front cover of recent issue) for price information. Deposit items may also be available on the American Mineralogist web site (<http://www.minsocam.org> or current web address).

**TABLE 4.** Selected interatomic distances and the angles of parasite-(Ce) (Å)

Ce1-F1	2.40(1)	Ce2-F1	2.39(1)	Ce3-F1	2.42(1)
Ce1-F2	2.42(1)	Ce2-F2	2.39(1)	Ce3-F2	2.39(1)
Ce1-F3	2.40(1)	Ce2-F3	2.37(1)	Ce3-F3	2.39(1)
mean	2.41	mean	2.38	mean	2.40
Ce1-O11	2.47(2)	Ce2-O13	2.57(2)	Ce3-O13	2.59(2)
Ce1-O23	2.60(2)	Ce2-O23	2.58(1)	Ce3-O21	2.49(2)
Ce1-O32	2.58(1)	Ce2-O31	2.50(2)	Ce3-O32	2.60(1)
Ce1-O42	2.60(2)	Ce2-O42	2.54(2)	Ce3-O41	2.58(2)
Ce1-O53	2.58(2)	Ce2-O51	2.59(2)	Ce3-O53	2.58(1)
Ce1-O61	2.57(1)	Ce2-O63	2.60(1)	Ce3-O63	2.54(1)
mean	2.57	mean	2.56	mean	2.56
Ce4-F4	2.39(1)	Ce5-F4	2.44(1)	Ce6-F4	2.39(1)
Ce4-F5	2.38(1)	Ce5-F5	2.37(1)	Ce6-F5	2.38(1)
Ce4-F6	2.39(1)	Ce5-F6	2.37(1)	Ce6-F6	2.45(1)
mean	2.39	mean	2.40	mean	2.41
Ce4-O43	2.59(2)	Ce5-O41	2.55(1)	Ce6-O43	2.57(2)
Ce4-O52	2.60(1)	Ce5-O52	2.55(2)	Ce6-O51	2.53(2)
Ce4-O61	2.56(1)	Ce5-O62	2.53(1)	Ce6-O62	2.60(1)
Ce4-O72	2.57(1)	Ce5-O72	2.55(1)	Ce6-O71	2.50(2)
Ce4-O81	2.52(2)	Ce5-O82	2.59(1)	Ce6-O82	2.63(1)
Ce4-O91	2.57(1)	Ce5-O92	2.53(1)	Ce6-O91	2.59(1)
mean	2.57	mean	2.55	Ce6-mean	2.57
Ca1-O12	2.40(1)	Ca2-O11	2.38(2)	Ca3-O12	2.49(2)
Ca1-O21	2.42(1)	Ca2-O12	2.78(2)	Ca3-O22	2.46(2)
Ca1-O22	2.85(2)	Ca2-O22	2.45(2)	Ca3-O31	2.37(1)
Ca1-O33	2.43(2)	Ca2-O33	2.49(2)	Ca3-O33	2.77(1)
Ca1-O73	2.37(1)	Ca2-O71	2.37(2)	Ca3-O73	2.43(1)
Ca1-O81	2.34(2)	Ca2-O73	2.74(1)	Ca3-O83	2.46(1)
Ca1-O83	2.69(1)	Ca2-O83	2.43(1)	Ca3-O92	2.38(1)
Ca1-O93	2.45(1)	Ca2-O93	2.45(1)	Ca3-O93	2.73(1)
mean	2.49	Ca2-mean	2.51	mean	2.51
C1-O11	1.34(3)	O11-O12	2.17(2)	O11-C1-O12	118(2)°
C1-O12	1.19(3)	O11-O13	2.16(2)	O11-C1-O13	115(2)°
C1-O13	1.22(3)	O12-O13	2.15(2)	O12-C1-O13	126(2)°
mean	1.25	mean	2.16	mean	120°
C2-O21	1.30(2)	O21-O22	2.20(2)	O21-C2-O22	121(2)°
C2-O22	1.23(3)	O21-O23	2.23(2)	O21-C2-O23	119(2)°
C2-O23	1.28(2)	O22-O23	2.18(2)	O22-C2-O23	120(2)°
mean	1.27	mean	2.20	mean	120°
C3-O31	1.26(2)	O31-O32	2.18(2)	O31-C3-O32	122(2)°
C3-O32	1.26(2)	O31-O33	2.17(2)	O31-C3-O33	116(1)°
C3-O33	1.31(2)	O32-O33	2.25(2)	O32-C3-O33	122(2)°
mean	1.28	mean	2.20	mean	120°
C4-O41	1.34(3)	O41-O42	2.22(2)	O41-C4-O42	116(2)°
C4-O42	1.29(3)	O41-O43	2.18(2)	O41-C4-O43	121(2)°
C4-O43	1.17(3)	O42-O43	2.15(2)	O42-C4-O43	123(2)°
mean	1.27	mean	2.18	mean	120°
C5-O51	1.27(2)	O51-O52	2.13(2)	O51-C5-O52	114(2)°
C5-O52	1.26(3)	O51-O53	2.20(2)	O51-C5-O53	121(2)°
C5-O53	1.26(3)	O52-O53	2.23(2)	O52-C5-O53	124(2)°
mean	1.26	mean	2.19	mean	120°
C6-O61	1.29(2)	O61-O62	2.17(2)	O61-C6-O62	115(2)°
C6-O62	1.29(2)	O61-O63	2.23(2)	O61-C6-O63	123(2)°
C6-O63	1.24(2)	O62-O63	2.22(2)	O62-C6-O63	122(1)°
mean	1.27	mean	2.21	mean	120°
C7-O71	1.28(2)	O71-O72	2.24(2)	O71-C7-O72	121(1)°
C7-O72	1.29(2)	O71-O73	2.19(2)	O71-C7-O73	114(2)°
C7-O73	1.33(2)	O72-O73	2.31(2)	O72-C7-O73	124(1)°
mean	1.30	mean	2.25	mean	120°
C8-O81	1.39(3)	O81-O82	2.25(2)	O81-C8-O82	119(2)°
C8-O82	1.21(2)	O81-O83	2.17(2)	O81-C8-O83	110(2)°
C8-O83	1.26(3)	O82-O83	2.25(2)	O82-C8-O83	131(2)°
mean	1.29	mean	2.22	mean	120°
C9-O91	1.24(3)	O91-O92	2.25(2)	O91-C9-O92	122(2)°
C9-O92	1.34(2)	O91-O93	2.29(2)	O91-C9-O93	128(2)°
C9-O93	1.31(3)	O92-O93	2.16(2)	O92-C9-O93	109(2)°
mean	1.30	mean	2.23	mean	120°

Note: Numbers in parentheses denote 1 esd of last unit cited.

phases are (001) layer structures. The crystal-structure refinements of bastnäsite-(Ce) (Ni et al. 1993) and synchysite-(Ce) (Wang et al. 1994) confirmed the layer nature of the minerals, and provided dimensions for all the component layers, (CeF), (Ca), (CO<sub>3</sub>), in the RE fluorcarbonates. These previous studies revealed that Ca and Ce (and other rare earth elements) exist in the vertical [001] columns, with a 4.11 Å repeat in (hexagonal) (001), regardless of the ratios of Ca- and Ce-bearing layers in the mineral or in domains of the layer intergrowth.

Figure 1 presents the polyhedral view of the parasite-(Ce) crystal structure. All Ce atoms coordinate to three fluorine atoms in the same (001) layer and six oxygen atoms, three from the neighboring (CO<sub>3</sub>) groups on each side. All Ca atoms coordinate with eight oxygen atoms, four from each adjoining (CO<sub>3</sub>) layer; the six shorter Ca-O bonds form a regular octahedron. The parasite-(Ce) structure consists of stacked (001) layers of the Ce polyhedra and Ca polyhedra. The polyhedra within the layers share edges, and the polyhedra between the layers are connected by apical oxygen atoms and by vertically oriented carbonate groups.

Figure 2 depicts the atomic arrangement of parasite-(Ce), with synchysite and bastnäsite for comparison. The (CeF), (CO<sub>3</sub>), and (Ca) layers in parasite-(Ce) are similar to the analogous layers in

synchysite-(Ce) and bastnäsite-(Ce) (Ni et al. 1993; Wang et al. 1994). The unit cell of parasite-(Ce) includes four (CeF) layers and two (Ca) layers with six intervening (CO<sub>3</sub>) layers. The (Ca) layers are positioned at  $z = 0$  and  $1/2$  to facilitate the comparison with synchysite. As in synchysite-(Ce), the intervening (CO<sub>3</sub>) layers are located slightly closer to the (Ca) layer than to the (CeF) layer, most likely because there is no anion in the (Ca) layer. The geometries of the (CO<sub>3</sub>) and (Ca) layers are essentially identical to those in synchysite-(Ce) (Wang et al. 1994). There is, however, a slight difference in the geometry of (CeF) layer. One of the three F atoms (F1 or F4) coordinated to Ce is almost at the (001) Ce plane, but other two are offset from the Ce plane by about 0.5 Å. The F atom closest to another (CeF) layer is offset from the (001) Ce plane by about 0.03 ≈ 0.05 Å more than the F atom that is closest to the (Ca) layer. This situation does not occur in synchysite because the (CeF) layer in synchysite is bonded above and below by (Ca) layers.

The parasite-(Ce) structure can be considered as two bastnäsite portions (each consists of a unit-cell thickness of bastnäsite, translated by  $\sim c/4$  from the traditional cell) connected by a (Ca) layer. Similarly, synchysite-(Ce) is composed of two bastnäsite portions [a bastnäsite unit cell lacking one (CeF) layer] linked by a (Ca) layer. In general, all fluorcarbonate phases can be envisioned as being composed of bastnäsite portions of different thickness, represented by the formula [(CeF)<sub>n</sub>(CO<sub>3</sub>)<sub>n+1</sub>], where  $n$  is an integer, that are linked by a (Ca) layer. Different types of linkages by the (Ca) layer results in polytypism both in parasite-(Ce) and synchysite-(Ce); many of these polytypes are enumerated in Yang et al. (1998).

The (Ca) layers are linked in the same way in parasite-(Ce) and the synchysite-(Ce) described by Wang et al. (1994). Although the bastnäsite portion [(CeF)<sub>2</sub>(CO<sub>3</sub>)<sub>3</sub>] in parasite-(Ce) possesses hexagonal symmetry, the stacked structure of the two bastnäsite portions linked by a (Ca) layer is no longer hexagonal. A structural offset between the bastnäsite portions is introduced by the intervening (Ca) layer, yielding monoclinic symmetry as in synchysite-(Ce) (Wang et al. 1994). In the bastnäsite structure, F atoms are in [001] columns along the triad and the average F-F distance along  $c^*$  is  $c/2$ , or 4.88 Å (Ni et al. 1993). In parasite-(Ce), because there is no corresponding F atom in the (Ca) layer, F-F distances in the F column would be as long as 9.11 Å, a large void created in the atomic arrangement without structural adjustments. Consequently, to close these voids, the bastnäsite portion above the (Ca) layer shifts in (001) by approximately 2.37 Å [or  $(a/6) \sin 60^\circ$ ] along  $[\bar{1}1\bar{0}]$  (or  $[1\bar{1}0]$  in the hexagonal cell; see solid arrows in Fig. 3). The next bastnäsite portion also shifts the same amount, along  $[1\bar{1}0]$  ( $[1\bar{0}0]$  in the hexagonal cell), which is  $120^\circ$  (or  $-120^\circ$ ) away from the previous shift direction, such that the oxygen atoms of the near-vertical edges of two overlaying CO<sub>3</sub> triangles will occupy the voids (Fig. 3). As a result of these shifts, the columns of F atoms in bastnäsite-(Ce) do not exist in parasite-(Ce), but are replaced by a column of ...F1, (CO<sub>3</sub> edge), (CO<sub>3</sub> edge), F2, F3, (CO<sub>3</sub> edge), (CO<sub>3</sub> edge), F3, F2, (CO<sub>3</sub> edge), (CO<sub>3</sub> edge), F1... in the stacking sequence along  $c^*$ . Thus, the triads are eliminated in parasite-(Ce) and no symmetry exists along  $c^*$ , yielding monoclinic symmetry. The shift of the structure portions along  $a$  in each unit cell can be calculated as  $2 \times (b/3) \cos 30^\circ = 4.11$  Å. From this layer offset,

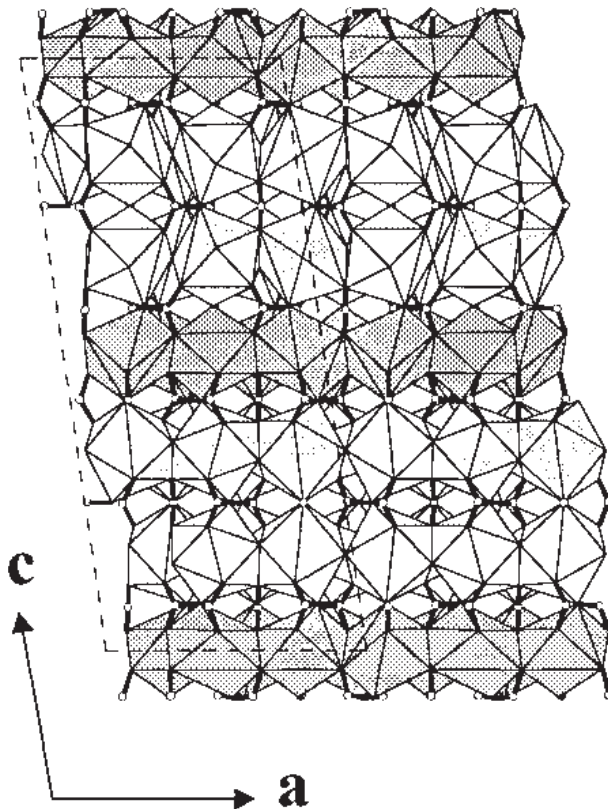
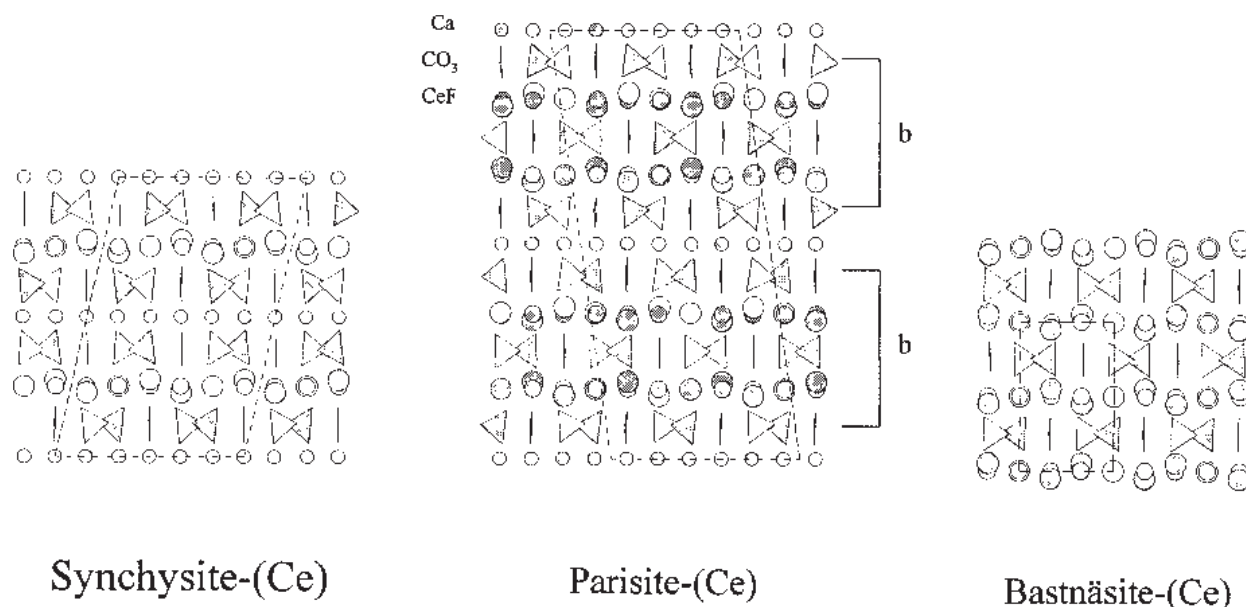


FIGURE 1. Polyhedral view of the atomic arrangement of parasite-(Ce) projected on (010). Atoms in carbonate groups are not depicted as polyhedra; the small circles represent C atoms, and the unit cell is outlined. Ca polyhedra are darker than RE polyhedra.



**FIGURE 2.** Atomic arrangement of parisite-(Ce) (p) projected on (010), with bastnäsite-(Ce) and synchysite-(Ce) for comparison. Triangles represent  $(\text{CO}_3)$  groups, and O atoms lie at the apices of the triangles. Circles from the largest to the smallest represent F, Ce, Ca, O, and C atoms, respectively. The unit cells are outlined. Bastnäsite-(Ce) layers in parisite are labeled “b” and Ca, CeF, and  $\text{CO}_3$  layers are denoted.

a  $\beta$  angle of  $90^\circ + \arctan(4.11 \text{ \AA}/c' \text{ \AA}) = 98.33^\circ$  can be calculated, in excellent agreement with the observed value of  $\beta$  of the monoclinic cell. Furthermore, because of the layer stacking sequence in parisite-(Ce), the twofold symmetry at  $z = 1/4$  is lost and the structure is accentric, *Cc*.

#### DISCUSSION OF THE STRUCTURE AND POLYTIPIISM

The atomic arrangement of “typical” parisite actually is very complicated and contains many polytypes that have been documented by XRD and TEM images. The polytypism in common parisite *sensu stricto*, as well as the existence of compositional variants with compositions between bastnäsite and synchysite, is controlled principally by the presence of syntactic intergrowths, as detailed below.

The RE fluorcarbonate layer structure, with (CeF) and  $(\text{CO}_3)$  common to all the RE fluorcarbonate phases, provides an identical growth surface amenable to crystallization of any of the RE fluorcarbonate phases as the fluid composition changes. Donnay and Donnay (1953) remarked that intergrowths are universal among the Ca fluorcarbonate minerals, even in euhedral single crystals, and later XRD and TEM studies confirmed that fact.

The pervasive existence of intergrowths in the RE fluorcarbonate phases allows the existence of many different domains (Donnay and Donnay 1953), or mixed-layer compounds, with composition between bastnäsite and synchysite [the compositions of the phases can be characterized as  $\text{B}_m\text{S}_n$ , with *m* bastnäsite (B) layers and *n* synchysite (S) layers; van Landuyt and Amelinckx 1975; Yang et al. 1994; therefore parisite is  $\text{B}_1\text{S}_1$ ] separated by structural or compositional “faults” in a single fluorcarbonate crystal. Tens of these compounds have been identified in previous TEM studies (van Landuyt and Amelinckx 1975; Yang et al. 1994; Wu et al. 1998). A domain can have different thickness,

from a few unit cells up to 0.1 mm. The result of XRD actually is the total diffraction by all the domains in the crystal; the intergrowths can be observed in [001] precession photographs.

Like other Ca fluorcarbonate phases such as synchysite-(Ce), different polytypes of parisite-(Ce) are known. Figure 3 is the crystal structure of parisite-(Ce) projected on (001), which helps to illustrate the cause of polytypism in parisite-(Ce) and in other Ca fluorcarbonate phases. As noted previously, the upper bastnäsite portion of the parisite structure shifts away (by  $a/3$ ) from the hexagonal position of the lower bastnäsite portion along [100] of the hexagonal cell to eliminate the voids created by insertion of the (Ca) layer in the F columns; the shift reduces the hexagonal symmetry to monoclinic. The solid arrows in Figure 3 denote these shifts in the monoclinic parisite-(Ce) structure. The vector of the upper shift is controlled by the lower shift,  $120^\circ$  away; thus there are two possible directions,  $120^\circ$  and  $240^\circ$ , that the upper shift can take. The shift directions could not be  $60^\circ$ , as in some of mica polytypes, because the oxygen atoms in the carbonate groups would appear in the same columns with the heavy atoms. The existence of two possible shift directions is one reason for the polytypism in parisite-(Ce). Such shifts occur in other fluorcarbonate domains that contain (Ca) layers, as well.

The cell thickness of parisite-(Ce) polytypes along  $c^*$  thus can be calculated as  $2n \times 14.1 \text{ \AA}$ , ( $n \geq 1$ );  $n = 1$  for the parisite-(Ce) structure given herein. Its polytype may be termed 2M, with thickness along  $c^* = 28.2 \text{ \AA}$ . In this manner, the other possible polytypes and the cell thickness also can be derived. One of the other possible polytypes is 6R, which possesses an hexagonal cell with  $c = 6 \times 14.1 \text{ \AA}$  (Fig. 3). The 6R polytype of parisite has long been considered as the most common one (Donnay and Donnay 1953). However, we did not find any other polytype of parisite other than 2M, after studying about ten perfect

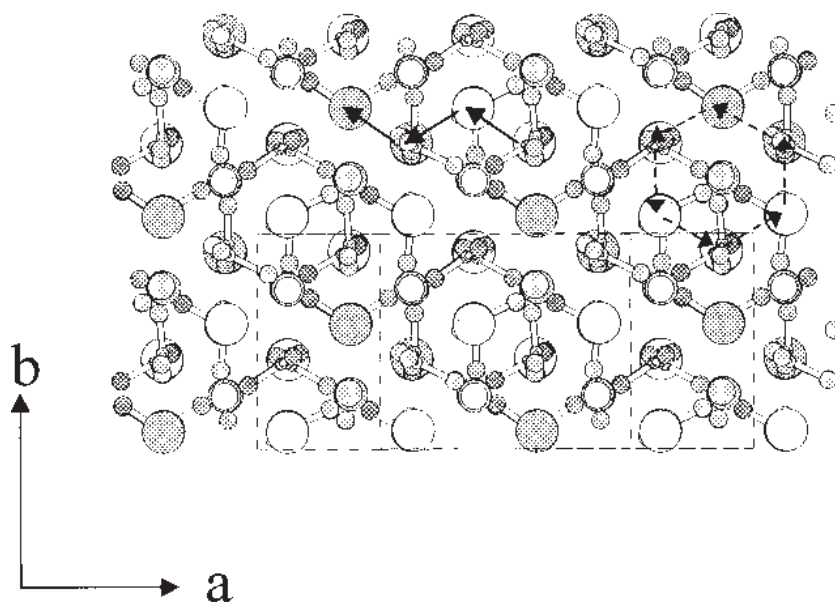


**FIGURE 3.** Atomic arrangement of parisite-(Ce) projected on (001). C-O bonds are depicted, and atomic symbols are the same as in Figure 1. Solid arrows indicate the shift direction of the bastnäsite portions in this structure with polytype 2M. Dotted arrows represent layer shifts in polytype 6R. Dashed line outlines the bottom of the unit cell, and fine line outlines the top of the unit cell.

crystals with the least intergrowth possible. It is reasonable to believe that the simplest polytype 2M is the most common one in parisite-(Ce).

It can be suggested that the 6R polytype mentioned in previous studies may actually be 2M, for two reasons. First, the previous studies did not recognize the possibility of the monoclinic symmetry and thus may not have evaluated that possibility.

Second, the TEM image studies revealed the diffraction pattern along only one  $a$  axis in the hexagonal cell, which may result in a 6R polytype with  $c = 6 \times 14.1 \text{ \AA}$  if assuming a hexagonal cell or may suggest a 3R polytype with  $c = 3 \times 14.1 \text{ \AA}$  if the diffraction pattern happened to be taken along the particular  $a$  axis that is actually a diad in a monoclinic cell. There is indeed an example where these two polytypes are recognized in a single parisite crystal (van Landuyt and Amelinckx 1975). If the diffraction of all the three  $a$ -axis directions had been examined for a homogeneous structure domain, these could have appeared unequal and suggested the monoclinic symmetry and the monoclinic polytype 2M.

In summary, the crystal structures of the fluorcarbonate phases can be described as structures composed of bastnäsite portions connected by a (Ca) layer, as shown in this work. This depiction can aid in understanding the fluorcarbonate structures. The bastnäsite crystal structure was elucidated (Ni et al. 1993), and is known to be without polytypism. The linkage of the (Ca) layer in other RE fluorcarbonates, however, will result in the structural offset of the bastnäsite portions away from hexagonal symmetry. With these two factors in the mind, the crystal structures of all fluorcarbonate phases or domains can be depicted, no matter how complicated the phase will be. The formula for the bastnäsite portion can be expressed as  $(\text{CeF})_n(\text{CO}_3)_{n+1}$ . In synchysite,  $n$  equals 1, in parisite  $n = 2$ , and  $n$  equals  $\infty$  in bastnäsite. For more complex

mixed-layer compounds or domains (Yang et al. 1994), there is more than one bastnäsite portion with different values of  $n$ . For instance, in röntgenite there are two bastnäsite portions,  $(\text{CeF})_1(\text{CO}_3)_2$  and  $(\text{CeF})_2(\text{CO}_3)_3$ . The different bastnäsite portions also could have different ratios in very complicated regularly stacked domains, such as  $\text{B}_{14}\text{S}_{15}$ , or  $\text{B}_{18}\text{S}_{10}$  (Yang et al. 1994). The domains can become very complicated, with extremely large unit cells.

The (Ca) layers can link two bastnäsite portions, but they cannot connect another (Ca) layer in natural fluorcarbonate minerals because such linkages will form a structure portion of vaterite (Meyer 1969; Kamhi 1963), which is not stable in normal geological conditions. Therefore, there is no fluorcarbonate phase found (Yang et al. 1994), even in microscopic scale, that has a composition containing more Ca than synchysite. Thus, synchysite should be the Ca-end of the fluorcarbonate mineral series.

#### ACKNOWLEDGMENTS

The authors are indebted to Joe Nelen for assisting in electron microprobe analysis and Tim Gooding for microprobe sample preparation. This study is supported by a Smithsonian Institution Postdoctoral Fellowship to Y.N. Earlier attempts at structure solution were supported by NSF grant EAR-9218577 to J.M.H. Editorial handling by Rodney C. Ewing and a detailed review by Joel D. Grice are sincerely appreciated.

#### REFERENCES CITED

- Brown, I.D. (1981) The bond-valence method: An empirical approach to chemical structure and bonding. In M. O'Keeffe and A. Navrotsky, Eds., *Structure and bonding in crystals II*, p. 1–30. Academic Press, New York.
- Donnay, G. and Donnay, J.D.H. (1953) The crystallography of bastnäsite, parisite, röntgenite and synchysite. *American Mineralogist*, 38, 932–963.
- Fair, C.K. (1990) MolEN, Structure Determination System. In MolEN, Program Descriptions. Enraf-Nonius, Delft, The Netherlands.
- Kamhi, S.R. (1963) On the structure of vaterite,  $\text{CaCO}_3$ . *Acta Crystallographica*, 16, 770–772.
- Main, P., Fiske, S.J., Hull, S.E., Lessinger, L., Germaine, G., Declercq, J.-P., and Woolfsong, M.M. (1980) MULTAN-80. A system of computer programs for the

- automatic solution of crystal structures from X-ray diffraction data. Universities of York, England and Louvain, Belgium.
- Meyer, H.J. (1969) Struktur und Fehlordnung des Vaterits. *Zeitschrift für Kristallographie*, 128, 183–212.
- Ni, Y., Hughes, J.M., and Mariano, A.N. (1993) The atomic arrangement of bastnäsite-(Ce),  $\text{Ce}(\text{CO}_3)\text{F}$ , and structural elements of synchysite-(Ce), röntgenite-(Ce), and parasite-(Ce). *American Mineralogist*, 78, 415–418.
- Oftedal, I. (1931a) Zur Kristallstruktur von Bastnäsit. *Zeitschrift für Kristallographie*, 78, 462–469.
- (1931b) Über Parisit, Synchisit und Kordylit. *Zeitschrift für Kristallographie*, 79, 437–464.
- van Landuyt, J. and Amelinckx, S. (1975) Multiple beam direct lattice imaging of new mixed-layer compounds of the bastnäsite-synchysite series. *American Mineralogist*, 60, 351–358.
- Walker, N. and Stuart, D. (1983) An empirical method for correcting diffractometer data for absorption effects. *Acta Crystallographica*, A39, 158–166.
- Wang, L., Ni, Y., Hughes, J.M., Bayliss, P., and Drexler, J.W. (1994) The atomic arrangement of synchysite-(Ce),  $\text{CeCa}(\text{CO}_3)_2$ . *The Canadian Mineralogist*, 32, 865–871.
- Wu, X., Yang, G., Meng D., and Pan, Z., Yang G. (1998) Transmission electron microscope study of new, regular, mixed-layer structures in calcium—rare-earth fluorcarbonate minerals. *Mineralogical Magazine*, 62, 55–64.
- Yang, G., Pan, Z., and Wu, X. (1994) Transmission electron microscope study of the new regular stacking structure in the calcium rare-earth fluorcarbonate mineral series from southwest China. *Scientia Geologica Sinica*, 29(4), 393–398 (Chinese with English abstract).
- Yang, Z., Tao, K. and Zhang, P. (1998) The symmetry transformations of modules in bastnaesite—vaterite polysomatic series. *Neues für Jahrbuch Mineralogie*, 1998, 1–12.

MANUSCRIPT RECEIVED MAY 3, 1999

MANUSCRIPT ACCEPTED SEPTEMBER 20, 1999

PAPER HANDLED BY RODNEY C. EWING